Development 140, 3395-3402 (2013) doi:10.1242/dev.097360


# Bmp signaling represses *Vegfa* to promote outflow tract cushion development

**Yan Bai[1,2], Jun Wang[1], Yuka Morikawa[1,3], Margarita Bonilla-Claudio[1], Elzbieta Klysik[1] and James F. Martin[1,2,3,4,5,*]**

## SUMMARY

Congenital heart disease (CHD) is a devastating anomaly that affects ~1% of live births. Defects of the outflow tract (OFT) make up a large percentage of human CHD. We investigated Bmp signaling in mouse OFT development by conditionally deleting both *Bmp4* and *Bmp7* in the second heart field (SHF). SHF *Bmp4/7* deficiency resulted in defective epithelial to mesenchymal transition (EMT) and reduced cardiac neural crest ingress, with resultant persistent truncus arteriosus. Using a candidate gene approach, we found that *Vegfa* was upregulated in the *Bmp4/7* mutant hearts. To determine if *Vegfa* is a downstream Bmp effector during EMT, we examined whether *Vegfa* is transcriptionally regulated by the Bmp receptor-regulated Smad. Our findings indicate that Smad directly binds to *Vegfa* chromatin and represses *Vegfa* transcriptional activity. We also found that *Vegfa* is a direct target for the miR-17-92 cluster, which is also regulated by Bmp signaling in the SHF. Deletion of *miR-17-92* reveals similar phenotypes to *Bmp4/7* SHF deletion. To directly address the function of *Vegfa* repression in Bmp-mediated EMT, we performed *ex vivo* explant cultures from *Bmp4/7* and *miR-17-92* mutant hearts. EMT was defective in explants from the *Bmp4/7* double conditional knockout (dCKO; *Mef2c-Cre;Bmp4/7*$^{f/f}$) and *miR-17-92* null. By antagonizing Vegfa activity in explants, EMT was rescued in *Bmp4/7* dCKO and *miR-17-92* null culture. Moreover, overexpression of *miR-17-92* partially suppressed the EMT defect in *Bmp4/7* mutant embryos. Our study reveals that *Vegfa* levels in the OFT are tightly controlled by Smad- and microRNA-dependent pathways to modulate OFT development.

**KEY WORDS: Bone morphogenetic protein, microRNA, Vascular endothelial growth factor A, Epithelial to mesenchymal transition, Outflow tract, Mouse**

## INTRODUCTION

Congenital heart disease (CHD) occurs in nearly 1% of all live births and is the leading cause of infant mortality and morbidity in the western world. Persistent truncus arteriosus (PTA) is the most severe phenotype of outflow tract (OFT) defects, with an unfavorable prognosis as surgical repair is not always possible (Williams et al., 1999). Although discovering the genetic causes would provide insight into the pathogenesis of CHD, the etiology of most human CHD, including OFT defects, remains unknown because of the multifactorial nature of the diseases, indicating the need for more study (Bruneau, 2008; Olson, 2006; Yamagishi et al., 2009; Zhao and Srivastava, 2007).

The OFT is derived from the second heart field (SHF), with a major contribution from cardiac neural crest (CNC) (Diman et al., 2011). The OFT, which first forms as a single tube, separates into the aorta and pulmonary trunk through both epithelial to mesenchymal transition (EMT) proximally and CNC influx into distal OFT. Endocardial cells in the proximal OFT undergo EMT and contribute to the proximal OFT cushions and to a subset of cells within semilunar valves. Defects in EMT and CNC influx are associated with several CHDs. During OFT development, endocardial cells sense and respond to inductive signals from overlying myocardium and initiate the process of EMT to contribute to conotruncal cushions. Several genes have been shown to regulate EMT, including *Twist1*, *Snai1* and *Slug* (*Snai2*) (Ma et al., 2005; Niessen et al., 2008; Yang et al., 2004).

Other studies show that Bmp signals are required for OFT morphogenesis (Liu et al., 2004; Ma et al., 2005; McCulley et al., 2008). *Bmp2* is involved in EMT during atrioventricular (AV) cushion development (Ma et al., 2005), whereas *Bmp4* is crucial for OFT separation and cushion development (Liu et al., 2004; McCulley et al., 2008). *Bmp4* mutant embryos show variability in phenotype with incomplete penetrance, possibly owing to the functional redundancy of Bmp ligands. Although ablation of *Bmp7* has no obvious phenotypic consequences in the heart (Solloway and Robertson, 1999), loss of *Bmp4* causes upregulation of *Bmp7* in OFT myocardium and compound mutants have a more severe phenotype (Liu et al., 2004). The overlapping expression of Bmp ligands in the OFT and their redundancy in function makes functional analysis of Bmp ligands in OFT development challenging.

Bmp signaling is transduced through a canonical pathway involving phosphorylation of Smad1/5/8 (R-Smad) from the ligand-receptor complex. Phosphorylated R-Smads then form a complex with Smad4 (Co-Smad) and this complex shuttles from cytoplasm to nucleus. Since Smads bind DNA motifs with low affinity and selectivity (Itoh et al., 2000; Karaulanov et al., 2004; Shi and Massagué, 2003; Zwijsen et al., 2003) they associate with various transcription factors to bind DNA and promote or repress transcription (Kawabata et al., 1998; Zwijsen et al., 2003).

Recent studies have shown that Bmp signaling also regulates downstream genes through microRNA (miRNA) maturation. In vascular smooth muscle, TGFβ- and Bmp-specific Smads are recruited to the p68 (Ddx5) RNA helicase-containing complex. The Smad-p68 complex interacts with the miRNA processing enzyme Drosha in the nucleus to regulate the biogenesis of a subset of

[1]Department of Molecular Physiology and Biophysics, Baylor College of Medicine, One Baylor Plaza, Houston, TX 77030, USA. [2]Institute of Biosciences and Technology, Texas A&M Health Science Center, Houston, TX 77030, USA. [3]Texas Heart Institute, Houston, TX 77030, USA. [4]Program in Developmental Biology, Baylor College of Medicine, One Baylor Plaza, Houston, TX 77030, USA. [5]Program in Genes and Development, University of Texas Graduate School of Biomedical Sciences, Houston, TX 77030, USA.

*Author for correspondence (jfmartin@bcm.edu)

**Accepted 7 June 2013**

miRNAs, including miR-21 (Davis et al., 2008). During cardiac development, *Bmp2/4* regulate OFT myocardial differentiation by promoting Smad-mediated transcription of the *miR-17-92* cluster (Wang et al., 2010). The *miR-17-92* cluster, which encodes miR-17, miR-18a, miR-19a, miR-20a, miR-19b-1 and miR-92-1, is oncogenic and also functions in the development of the heart, lungs and immune system (Koralov et al., 2008; Ventura et al., 2008; Vincentz et al., 2008; Xiao et al., 2008).

In this study, we discovered that loss of *Bmp4/7* in the SHF resulted in PTA with upregulation of *Vegfa*, repression of which is required in the atrioventricular canal (AVC) to promote EMT (Chang et al., 2004). Our *in vitro* studies showed that *Vegfa* is repressed by both Smad and miR-17/20a. Moreover, *in vivo* and *ex vivo* studies showed that overexpression of *miR-17-92* or repression of *Vegfa* can partially suppress the Bmp loss-of-function phenotype. Our study reveals that in the OFT, EMT and CNC influx are regulated by Bmp via a combination of Smad- and miRNA-dependent *Vegfa* repression.

## MATERIALS AND METHODS

### Mouse lines

The *Bmp4* flox, *miR-17-92* null and *miR-17-92*$^{OE}$ alleles and *Mef2c-Cre* lines have been described previously (Liu et al., 2004; Ventura et al., 2008; Verzi et al., 2005; Xiao et al., 2008). To generate the *Bmp7* flox allele, a targeting vector was constructed that introduced one loxP site upstream of *Bmp7* exon 4 followed by an FRT-flanked PGKneo cassette, while another loxP site was introduced downstream of *Bmp7* exon 4 (see supplementary material Fig. S1).

### β-galactosidase staining, histology and immunostaining

Embryos were fixed overnight in 4% paraformaldehyde or buffered formalin, dehydrated through a graded ethanol series, and paraffin embedded. Sections were cut at 7 μm and used for Hematoxylin and Eosin (H&E) staining or immunostaining. Detection of *lacZ* expression on whole embryos was performed as previously described (Lu et al., 1999). For Twist1 immunodetection, sections were deparaffinized and hydrated. For antigen retrieval, 10 mM citrate buffer was used. Monoclonal anti-Twist1 (Abcam, ab50887; 1:200) was used as primary antibody. HRP-conjugated anti-mouse secondary antibody (Bio-Rad) was visualized using TSA Plus Fluorescence Systems (PerkinElmer). Nuclei were stained with 4′,6-diamidino-2-phenylindole dihydrochloride (DAPI) (Invitrogen).

### Quantitative real-time RT-PCR

Total RNA from OFT (E10.5 embryos) was isolated using the RNeasy Micro Kit (Qiagen). SuperScript II reverse transcriptase (Invitrogen) was used for reverse transcription (RT)-PCR with 20-100 ng mRNA and SYBR Green JumpStart Taq ReadyMix (Sigma) in triplicate reactions on a StepOnePlus Real-Time PCR System (ABI); *Gapdh* was used as internal control. *Vegfa* was detected by TaqMan probe (IDT, Mm.PT.47.7135538.g) with 18s rRNA (IDT) as internal control. For miRNAs, TaqMan MicroRNA Assay Kits (Applied Biosystems) were used according to the manufacturer's guidelines. *Sno-202* was used as internal control. For all qRT-PCR experiments, at least four mutant and four control embryos were analyzed. All error bars represent s.e.m. Primer sequences are available in supplementary material Table S1.

### Sequence analysis and miRNA target prediction

For sequence analysis and alignment, NCBI (http://www.ncbi.nlm.nih.gov/), Ensemble (http://uswest.ensemble.org/index.html), rVista 2.0 (http://rvista.dcode.org/) and TFSEARCH (http://mbs.cbrc.jp/research/db/TFSEARCH.html) were used. For miRNA target prediction, miRanda (http://www.microrna.org), TargetScan (http://www.targetscan.org) and miRDB (http://mirdb.org/miRDB/) were used.

### Generation of constructs

To generate the *Vegfa* promoter luciferase reporter plasmid, a 1563 bp fragment of the mouse *Vegfa* promoter was amplified using a high-fidelity PCR system (Roche) and subcloned into the pGL3-Basic vector (Promega). To generate the *Vegfa* 3′UTR luciferase reporter plasmid, 1881 bp of *Vegfa* 3′UTR genomic sequence was amplified using the high-fidelity PCR system from a cDNA clone (#6816435, Open Biosystems) and subcloned into the pMIR-REPORT Luciferase miRNA Expression Reporter Vector (Ambion). Site-directed mutagenesis of the seed sites in the *Vegfa* 3′UTR and *Vegfa* promoter was performed with the QuickChange II Site-Directed Mutagenesis Kit (Stratagene). Primers are listed in supplementary material Table S1.

### Luciferase activity assay

P19 cells were transfected with the *Vegfa* promoter and 3′UTR reporter plasmids described above using Lipofectamine 2000 (Invitrogen). Luciferase activity assays were performed using the Dual-Luciferase Reporter Assay System (Promega). The Renilla luciferase-encoding plasmid pRL-TK was used as the normalization control. Ca-Alk3 (Wang et al., 2010) was used to activate the Smad pathway. miRNA mimics were purchased from Thermo Scientific.

### *Ex vivo* OFT explant culture

A solution (1.5 mg/ml) of rat tail collagen type I (BD Biosciences) was dispensed into 24-well microculture dishes and allowed to solidify in a 37°C, 5% $CO_2$ incubator. Collagen gels were washed several times with DMEM containing 10% fetal bovine serum (FBS), 0.1% insulin-transferrin-selenium (ITS, Gibco, Invitrogen) and 100 unit/ml penicillin, 100 μg/ml streptomycin (1:100, penicillin-streptomycin solution, Hyclone, Thermo Scientific). OFTs were harvested in sterile Tyrode's Salt Solution (Sigma-Aldrich) from E10.5 embryos. OFTs were carefully dissected, and endocardium was exposed to the collagen gel, with the myocardium overlaying. Four hours after attachment, medium (100 μl/well) was added and explants cultured for up to 3 days. Explants were fixed and stained with anti-alpha-SMA-Cyan3 (1:100; Sigma-Aldrich) to detected mesenchymal cells and phalloidin-FITC (1:100; Sigma-Aldrich) to reveal the actin cytoskeleton as described (Luna-Zurita et al., 2010). TO-PRO-3 Iodide (TOP3; Invitrogen) was used for nuclei staining. For explant treatments, the medium was supplemented with sFlt (10 ng/ml; R&D Systems, 471-F1). Medium was replaced every 24 hours.

### *In vivo* chromatin immunoprecipitation

About 80 OFTs of E10.5 wild-type embryos were dissected and subjected to chromatin immunoprecipitation (ChIP) analysis. Soluble chromatin was prepared after formaldehyde crosslinking and sonication. Smad1/5/8 antibody (sc-6031 X, Santa Cruz) was used to immunoprecipitate protein-bound DNA fragments; rabbit IgG was used as control. The PCR products for the SBE1, SBE2 and SBE3 fragments are 280 bp, 402 bp and 204 bp, respectively. Primers that amplified sequence irrelevant for Smad binding were used as a negative control. SYBR Green was used for ChIP-qPCR, and results were analyzed by the percentage input method (Invitrogen). Primer sequences are available in supplementary material Table S1.

## RESULTS

### Bmp2, Bmp4 and Bmp7 regulate EMT and have redundant functions

Bmp2, Bmp4 and Bmp7 show overlapping expression patterns and functional redundancy (Bonilla-Claudio et al., 2012; Dudley and Robertson, 1997; Furuta et al., 1997; Wang et al., 2010). We compared their expression patterns using *lacZ* knock-in mouse lines for *Bmp2* and *Bmp4* and *in situ* hybridization of *Bmp7*. *Bmp2* and *Bmp4* were expressed in the OFT at E9.5, whereas *Bmp7* was broadly expressed throughout the heart tube (supplementary material Fig. S2A,B,G,H,M,N). *Bmp4* expression was found in the inflow tract at E9.5, but was limited to the OFT at E10.5. Analysis of the sections revealed that *Bmp2*, *Bmp4* and *Bmp7* were exclusively co-expressed in OFT myocardium (supplementary material Fig. S2C,E,I,L,O,R). At E10.5, expression of *Bmp2* in the OFT was decreased (supplementary material Fig. S2G,J), whereas *Bmp4* and *Bmp7* expression was maintained at similar levels (supplementary material Fig. S2A,D,M,P).

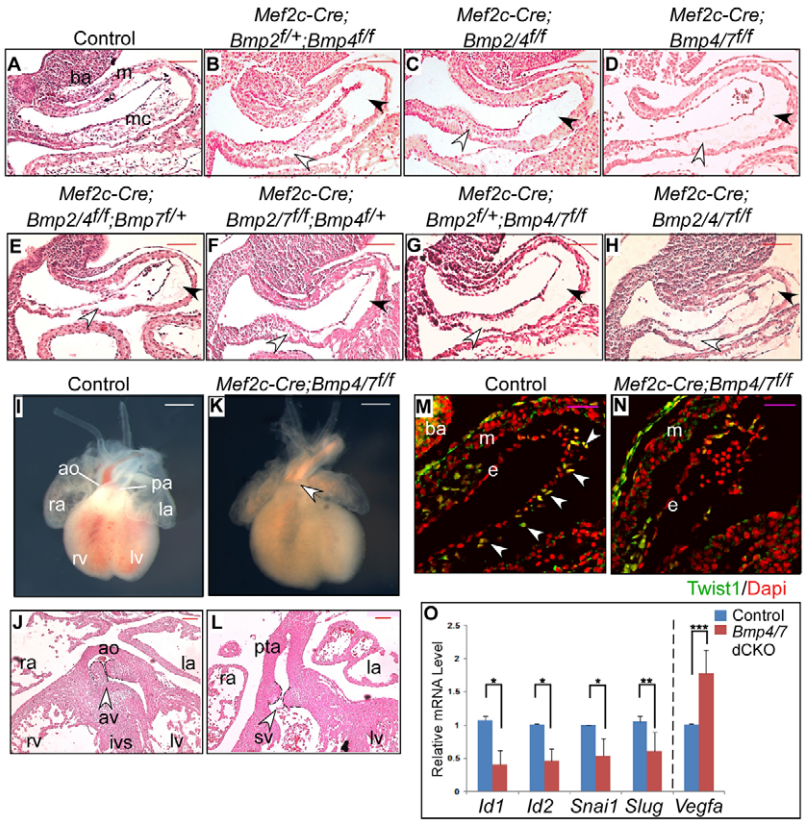


**Fig. 1. Inactivation of *Bmp2*, *Bmp4* and *Bmp7* in the SHF.** (**A-H**) Hematoxylin and Eosin-stained sagittal sections of E10.5 mouse embryos with different combinations of Bmp gene deletion. The Bmp genes were knocked out conditionally in the second heart field (SHF) using *Mef2c-Cre*. Black arrowheads indicate proximal outflow tract (OFT) and white arrowheads distal OFT. For A-H, *n*=6, 5, 5, 6, 3, 2, 5, 5. (**I-L**) Whole-mount (I,K) and sections (J,L) of control and *Bmp4/7* dCKO hearts at E14.5. The arrowhead in K indicates persistent truncus arteriosus (PTA). ba, branchial arch; m, myocardium; mc, mesenchymal cushion; e, epithelium; ao, aorta; pa, pulmonary artery; la, left atrium; ra, right atrium; lv, left ventricle; rv, right ventricle; av, aorta valve; sv, semilunar valve; pta, persistent truncus arteriosus; ivs, interventricular septum. (**M**,**N**) Immunostaining of Twist1 in control and *Bmp4/7* dCKO embryos at E10.5. Arrowheads point to Twist1-positive cells. (**O**) The expression of EMT-related genes was examined in the OFT of control and *Bmp4/7* dCKO embryos at E10.5. RT-PCR analysis was performed using SYBR Green for *Id1/2*, *Snai1* and *Slug* and TaqMan for *Vegfa*. Control, *n*=5; mutant, *n*=4. Error bars represent s.e.m. **P*<0.004, ***P*=0.03, ****P*=0.04 (two-tailed *t*-test). Scale bars: 100 μm in A-I,K; 500 μm in J,L; 50 μm in M,N.

To examine functional redundancy, we deleted *Bmp2*, *Bmp4* and *Bmp7* in different combinations in the OFT using *Mef2c-Cre* (Fig. 1A-H). Proximal OFT mesenchymal cells were absent from *Bmp2/4*, *Bmp4/7* and *Bmp2/7* double conditional knockout (dCKO) embryos (Fig. 1C-F). *Bmp4/7* deletion resulted in OFT cushion defects in CNC-derived distal OFT, as well as proximal OFT (Fig. 1D). The distal OFT defects were not observed upon deleting *Bmp2* in a *Bmp4* homozygous or heterozygous background, suggesting that *Bmp2* has limited function in the OFT proper (Fig. 1C,F).

Consistent with the defective CNC influx and proximal EMT observed at E10.5, *Bmp4/7* mutants had severe OFT defects at E14.5, with failure of OFT separation resulting in PTA (Table 1, Fig. 1I-L). One *Bmp4/7* dCKO embryo had double outlet right ventricle (DORV), with both aortic and pulmonary arteries draining the right ventricle (Table 1). In addition to defective great vessel separation, histological sections revealed hypoplastic semilunar valves and an interventricular septal defect (VSD; data not shown) in the *Bmp4/7* dCKO (Fig. 1J,L). Taken together, our findings revealed that *Bmp4* and *Bmp7* have redundant functions in OFT development. To further explore Bmp signaling in the OFT, we focused on the *Bmp4/7* dCKO mouse model.

**Table 1. OFT defects in *Bmp2/4/7* conditional knockout embryos at E14.5**

| Genotype | PTA | DORV |
|---|---|---|
| *Mef2c-Cre;Bmp4/7$^{f/f}$* | 6/7 | 1/7 |
| *Mef2c-Cre;Bmp2$^{f/+}$Bmp4/7$^{f/f}$* | 5/5 | n/a |
| *Mef2c-Cre;Bmp2/4/7$^{f/f}$* | 6/6 | n/a |

The frequency of persistent truncus arteriosus (PTA) and double outlet right ventricle (DORV) among total embryos examined is shown for each genotype. n/a, not applicable.

To investigate EMT in the *Bmp4/7* dCKO, we performed phosphohistone H3 (pHH3) analysis for cell proliferation and did not observe any obvious difference between the control and *Bmp4/7* dCKO in the myocardium (data not shown). Immunostaining showed fewer Twist1-expressing mesenchymal cells in the OFT of the *Bmp4/7* dCKO than the control (Fig. 1M,N), indicating that fewer cells progressed through EMT in the *Bmp4/7* mutant. To determine the mechanism of EMT regulation by Bmp, the expression of genes involved in the Bmp pathway and EMT was examined by qRT-PCR. The Bmp-regulated EMT genes *Snai1*, *Slug*, *Id1* and *Id2* were significantly decreased in the *Bmp4/7* dCKO OFT, whereas *Vegfa* was upregulated 1.8-fold (Fig. 1O).

## Smad directly represses *Vegfa* transcription

The major downstream Bmp signaling effectors are Smad proteins. To determine whether *Vegfa* is a direct downstream target of Bmp, we searched for conserved Smad binding sites in *Vegfa* upstream sequences by bioinformatics analysis. Analysis of *Vegfa* upstream sequence predicted several conserved functional elements for the Bmp response (McCulley et al., 2008), comprising Smad binding elements (SBEs) and the Smad1 binding motif (s1). The SBE is a canonical Smad binding sequence (Shi et al., 1998) that is found in the promoter of many TGFβ- and Bmp-responsive genes, whereas the s1 motif is found in the promoter of *Xenopus vent2*. These motifs are usually flanked by Bmp responsive element (BRE)-like and/or GC-rich boxes (Fig. 2A), which are common in the regulatory elements of Bmp-responsive genes. To test whether Smad directly binds *Vegfa* upstream sequences, we performed *in vivo* chromatin immunoprecipitation (ChIP)-PCR analysis on wild-type E10.5 OFT. We detected enrichment in the anti-Smad1/5/8 ChIP-PCR for all three putative SBEs (Fig. 2B,C). ChIP-qPCR data further supported that these putative SBEs were bound by Smad in *Vegfa* chromatin

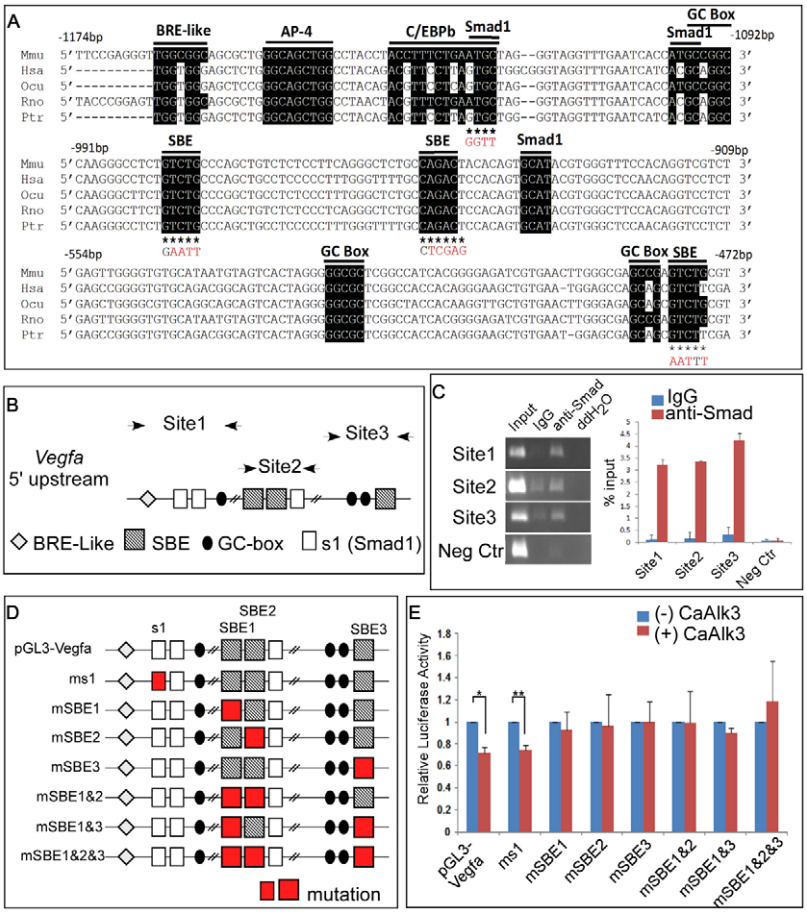


**Fig. 2. Transcriptional modulation of *Vegfa* by Smad.** (**A**) Putative transcription factor/Smad binding sites in the *Vegfa* upstream sequence from mouse (Mmu), human (Hsa), chimpanzee (Ptr), rat (Rno) and rabbit (Ocu). Mutations introduced into the *Vegfa* promoter in the luciferase reporters are shown in red. (**B**) *Vegfa* upstream sequence illustrating the positions of ChIP primers (arrows). s1, Smad1 binding motif; SBE, Smad binding element. (**C**) *In vivo* ChIP indicates that Smad is bound to *Vegfa* chromatin. DNA from wild-type OFT was immunoprecipitated with antibody against Smad1/5/8. Non-specific rabbit IgG was used as negative control. Non-immunoprecipitated DNA (10% input) was used as positive control. PCR analysis employed the primer sets shown in B. $ddH_2O$, PCR in the absence of template DNA. The bar chart shows the percentage input immunoprecipitated by IgG and anti-Smad as assessed by ChIP-qPCR. Each sample is in triplicate. (**D**) Native and mutated *Vegfa* reporter constructs. (**E**) Luciferase assay. Native and mutated *Vegfa* reporter constructs were transfected with or without the constitutively active ca-Alk3 construct. **P*=0.011, ***P*=0.009 (two-tailed *t*-test). All error bars represent s.e.m.

(Fig. 2C). These results indicate that Smad1/5/8 can directly bind *Vegfa* chromatin in the OFT.

To determine whether Smad directly regulates *Vegfa* transcription, we cloned a ~1500 bp region upstream of *Vegfa* and generated a luciferase reporter (Fig. 2D). To activate the Smad-dependent Bmp pathway, we co-transfected a constitutively active form of the type 1 Bmp receptor Alk3 (ca-Alk3) into the mouse P19 cell line (Wang et al., 2010) (Alk3 is also known as Bmpr1a – Mouse Genome Informatics). Luciferase assays demonstrated that *Vegfa* promoter activity was significantly diminished, by 35%, in the presence of ca-Alk3 (Fig. 2E). To determine whether *Vegfa* promoter repression was due to direct Smad binding, we introduced mutations into the predicted Smad binding sites (Fig. 2D). Mutations in SBE1, SBE2 and/or SBE3 resulted in loss of repression by Bmp signaling (Fig. 2E), showing that Smad directly binds these sites and represses *Vegfa*. Mutation in s1 did not affect luciferase activity (Fig. 2E), suggesting that this motif is not necessary in repressing *Vegfa*. These results indicated that Smad can directly repress *Vegfa* transcription, but by only 35%. Since loss of *Bmp4/7* resulted in a 175% increase in *Vegfa* levels, there might be other important Smad elements that are excluded from our luciferase reporter or other Bmp downstream effector mechanisms that contribute to *Vegfa* regulation.

## miR-17 and miR-20a are downstream effectors of Bmp in *Vegfa* repression

Our results raise the possibility that *Vegfa* levels are regulated by mechanisms other than direct Smad binding to *Vegfa* chromatin. Alternative downstream Bmp effectors include miRNAs, which are involved in the refinement of gene expression. *miR-17-92* is downstream of the Bmp pathway in cardiac development (Wang et al., 2010). Bioinformatic analysis predicted a highly conserved miR-17/20a binding site in the 3′UTR of *Vegfa* (Fig. 3A). The levels of pri-miR-17-92 and mature miR-17/20a were decreased in the OFT of *Bmp4/7* dCKO embryos (Fig. 3B), showing that *miR-17/20a* are downstream of Bmp4/7.

To determine the role of miR-17-92 during OFT development, we analyzed *miR-17-92* null (*miR-17-92*$^{N/N}$) embryos. At E10.5, *miR-17-92*$^{N/N}$ embryos showed OFT defects, including lack of mesenchymal cushion formation (Fig. 3C,D). *miR-17-92*$^{N/N}$ embryos developed no mesenchymal cells in either the proximal or distal OFT, resembling the phenotype of the *Bmp4/7* dCKO. At E14.5, *miR-17-92*$^{N/N}$ embryos exhibited the DORV phenotype, together with abnormal semilunar valve and VSD (Fig. 3E,F). Notably, loss of *miR-17-92* resulted in a 1.7-fold increase in the level of *Vegfa* (Fig. 3G). This upregulation of *Vegfa* is similar to that observed in the *Bmp4/7* dCKO (Fig. 1O). Taken together, our results suggest that *miR-17-92* is downstream of Bmp signaling during EMT in the OFT.

To determine whether *Vegfa* can be regulated by miR-17 and miR-20a, we cloned 1874 bp of the native *Vegfa* 3′UTR and constructed a luciferase reporter vector (Fig. 3H). Co-transfection with *miR-17/20a* resulted in suppression of the *Vegfa* 3′UTR reporter (Fig. 3I), whereas *miR-92a* did not suppress the luciferase activity. Then we mutated the miR-17/20a binding site in the *Vegfa* 3′UTR (Fig. 3H). Suppression by both miR-17 and miR-20a was abolished in the mutated *Vegfa* reporter (Fig. 3I), showing that the putative miR-17/20a site was responsible for 3′UTR silencing of

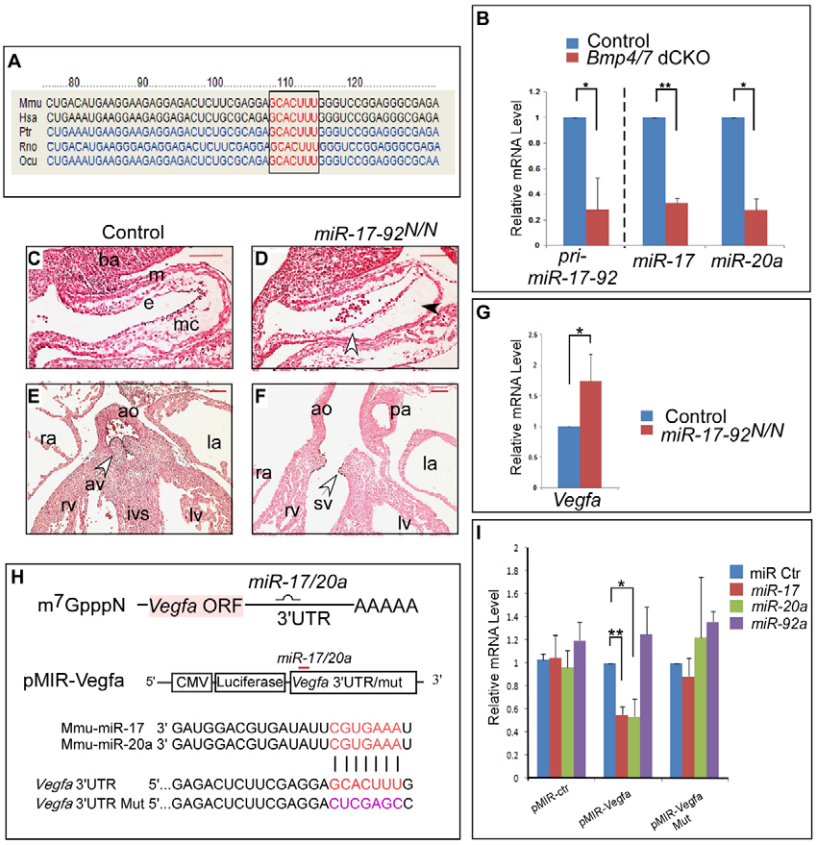


**Fig. 3. miR-17/20a are downstream effectors of Bmp signaling.** (**A**) Analysis of the *Vegfa* 3′UTR reveals a highly conserved miR-17/20a binding site (boxed). Species abbreviations as Fig. 2. (**B**) qRT-PCR analysis of pri-miR-17-92, miR-17 and miR-20a in the OFT of *Bmp4/7* dCKO mouse embryos. **P*=0.049, ***P*=0.027 (two-tailed *t*-test). Control, *n*=5; mutant, *n*=3. (**C-F**) Histological analysis of *miR-17-92* null embryos at E10.5 (C,D) and E14.5 (E,F). Black arrowhead indicates a proximal EMT defect at E10.5 (D). White arrowheads indicate a distal EMT defect (D) and abnormal semilunar valve at E14.5 (F). See Fig. 1 for labels. (**G**) qRT-PCR analysis of *Vegfa* in the OFT of the *miR-17-92* mutant. Control, *n*=4; mutant, *n*=4. **P*=0.046 (two-tailed *t*-test). (**H**) (Top) Binding of miR-17/20a seed sequences to the *Vegfa* 3′UTR. (Middle) *Vegfa* 3′UTR luciferase reporter construct. (Bottom) Mutation of seed sequences. (**I**) Luciferase assay performed by transfecting reporter construct and *miR-17* or *miR-20a*. *miR-92a* was used as a negative control. **P*=0.032, ***P*=0.009 (two-tailed *t*-test). All error bars represent s.e.m.

*Vegfa*. These results strongly suggest that miR-17/20a are downstream effectors of Bmp4/7 in repression of *Vegfa*.

## Repression of *Vegfa* regulates EMT during OFT development

Vegfa is known to inhibit mesenchymal transformation in the AV cushion (Chang et al., 2004); however, the potential roles of Vegfa in EMT during Bmp-mediated OFT development have not been investigated. To determine if Bmp regulates EMT through *Vegfa* repression, we investigated whether reducing Vegfa can rescue the EMT defect caused by *Bmp4/7* deletion. We performed *ex vivo* analysis by culturing the OFT from E10.5 embryos on collagen gel, with the endocardium exposed to the gel (Fig. 4A). In control explants, a halo of mesenchymal cells formed around the myocardium, with non-invasive mesenchymal cells on the surface of the gel and invasive mesenchymal cells invading the collagen depths (Fig. 4B,C). In the OFT of the *Bmp4/7* dCKO, both invasive and non-invasive EMT were absent (Fig. 4D,E). Administration of sFlt (Flt1 – Mouse Genome Informatics), a soluble Vegfa antagonist, partially suppressed the mesenchymal transformation defect in the *Bmp4/7* dCKO by rescuing non-invasive mesenchyme cell formation (Fig. 4F). Invasive EMT was not rescued by antagonizing *Vegfa* (Fig. 4G), suggesting that this process is regulated by other downstream Bmp targets, such as *Snai1*.

Next, to determine whether miR-17 and miR-20a regulate EMT through *Vegfa*, we performed explant culture from *miR-17-92*$^{N/N}$ OFT (Fig. 4H,I). The OFT from the *miR-17-92* null lacked both invasive and non-invasive EMT (Fig. 4H,I), recapitulating the explant from the *Bmp4/7* dCKO (Fig. 4D). After addition of the Vegfa antagonist sFlt to the explant, both the non-invasive and invasive EMT processes were rescued in the *miR-17-92*$^{N/N}$ explants (Fig. 4J,K), showing that *Vegfa* downregulation was sufficient to rescue the *miR-17-92* loss-of-function phenotype. Since antagonizing Vegfa was not sufficient to rescue invasive EMT in the explant from the *Bmp4/7* dCKO (Fig. 4G), regulation of *Vegfa* by miR-17-92 must be just one of multiple downstream effectors of Bmp signaling.

## *miR-17-92* can rescue defects in EMT caused by loss of Bmp

To address the hypothesis that miR-17/20a are direct downstream effectors of Bmp in the EMT process *in vivo*, we overexpressed *miR-17-92* in the *Bmp4/7* dCKO by crossing *miR-17-92*$^{OE/+}$ (Xiao et al., 2008) and *Mef2c-Cre* lines. qRT-PCR data showed that miR-17 and miR-20a were mildly elevated, by ~1.3-fold, in the OFT of *Mef2c-Cre;miR-17-92*$^{OE/+}$ embryos (Fig. 5A). *Vegfa* levels were moderately downregulated in the OFT of *Mef2c-Cre;miR-17-92*$^{OE/+}$ (Fig. 5A), demonstrating that miR-17-92 represses *Vegfa in vivo*. To determine whether *miR-17-92* can compensate for the loss of *Bmp4/7*, we generated *Mef2c-Cre;Bmp4/7*$^{f/f}$*;miR-17-92*$^{OE/+}$ embryos. Mesenchymal cushion formation was observed in the OFT of *Mef2c-Cre;Bmp4/7*$^{f/f}$*;miR-17-92*$^{OE/+}$ embryos (Fig. 5E,F): proximal cushion-forming cells were observed in 83% of the embryos, whereas distal cushion cells were observed in all embryos examined (Table 2). At E14.5, the valve defect of *Bmp4/7* dCKO embryos was rescued by overexpression of *miR-17-92*, and OFT septation was partially rescued in the distal part (data not shown). The level of *Vegfa* in *Mef2c-Cre;Bmp4/7*$^{f/f}$*;miR-17-92*$^{OE/+}$ embryos was decreased compared with *Mef2c-Cre;Bmp4/7*$^{f/f}$ and comparable to that of control embryos (Fig. 5B), suggesting that suppression of *Vegfa* by Bmp was mediated by miR-17 and miR-20a. These results strongly suggest that miR-17 and miR-20a are downstream effectors of the Bmp signal during OFT development.

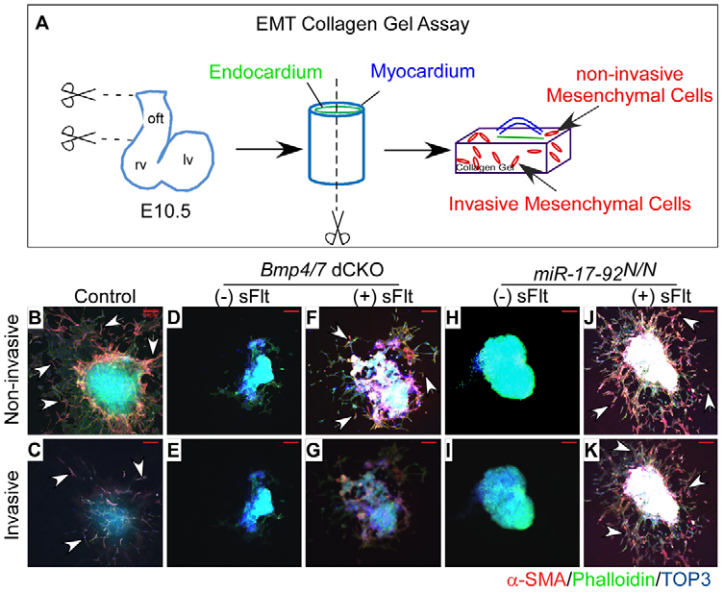


**Fig. 4. *Ex vivo* collagen gel assay of EMT in the OFT.** (**A**) Outline of the OFT explant culture on collagen gel. The OFT from an E10.5 mouse embryo was dissected, cut, and placed on the collagen gel. The inner endocardium layer (green) was exposed to the gel, with the myocardium (blue) on the top. lv, left ventricle; rv, right ventricle; oft, outflow tract. (**B-K**) EMT assays on the OFT of control, *Bmp4/7* dCKO, and *miR-17-92* null embryos in the presence or absence of the Vegfa antagonist sFlt. EMT was visualized by phalloidin to outline the cell shape and by alpha-SMA immunostaining to stain mesenchymal cells. TOP3 was used to stain nuclei. Invasive EMT is observed on the surface of the collagen gel (top row, arrowheads) and non-invasive EMT is observed in the gel (bottom row, arrowheads). Scale bars: 100 μm.

Although cushion formation was observed in *Mef2c-Cre;Bmp4/7$^{f/f}$;miR-17-92$^{OE/+}$* embryos, there were fewer mesenchymal cushion-forming cells in the rescued embryos, indicating partial suppression (Fig. 5C-F). In addition, the extent of mesenchymal cushion formation was variable (Fig. 5C-F, Table 2). Together, these data support the hypothesis that Bmp signals are mediated by effector mechanisms in addition to miR-17.

## DISCUSSION

Our data uncover a direct interaction between the Bmp and Vegfa signaling pathways that are important for normal OFT development. Moreover, our findings uncover a mechanism to tightly modulate Vegfa activity levels in the OFT. Our results also provide new insight into the mechanism for coordinated development of CNC and endocardial cells as they contribute to the conotruncal cushions. Lastly, our data reveal that miR-17-92 indirectly, via non-cell-autonomous mechanisms, regulates CNC development in addition to that of SHF-derived tissues.

### Coordinated regulation of cushion formation derived from multiple cell types

The conotruncal cushions are derived from both CNC and the endocardium. Bmp signaling has been implicated previously in EMT within the AVC. We now show that Bmp signaling is also important for EMT within the OFT. Previous data in the AVC indicate that Bmp regulates genes such as *Twist* and *Snai1* to promote EMT and, although we did not focus on that mechanism here, it is likely that similar mechanisms are at work in both the OFT and AVC. Our finding that Bmp signaling negatively regulates *Vegfa* in the OFT provides important insight into the coordinated regulation of the OFT cushions. In the OFT, in contrast to the AVC, there are three separate tissues developing in close proximity: myocardium, endocardium and CNC. We provide evidence that *Vegfa* repression mediated by Bmp–miR-17-92 is a crucial mechanism to ensure coordinated OFT development.

The importance of Vegf signaling in endocardium has recently been demonstrated. Deleting the Vegf receptor neuropilin 1 (*Nrp1*)

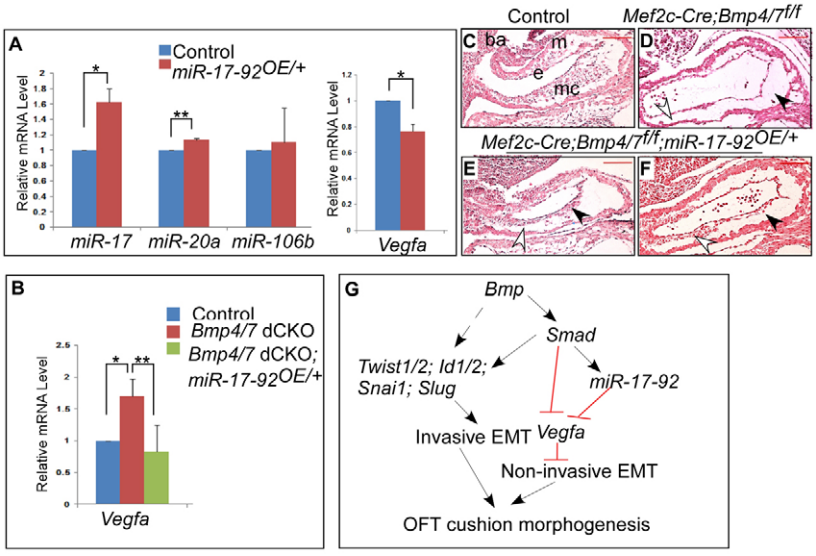


**Fig. 5. Rescue of *Bmp4/7* deficiency by conditionally overexpressing *miR-17-92*.** (**A**) qPCR analysis of miR-17, miR-20a and *Vegfa* expression in the OFT of *miR-17-92$^{OE/+}$* mouse embryos. miR-106b is used as a negative control. *$P$=0.016 (miR-17), *$P$=0.047 (*Vegfa*), **$P$=0.033 (two-tailed *t*-test). Control, $n$=4; mutant, $n$=4. (**B**) qRT-PCR analysis of *Vegfa* expression in *Bmp4/7* dCKO and *miR-17-92$^{OE/+}$* embryos. Control, $n$=6; *Bmp4/7* mutant, $n$=5; *miR-17-92* mutant, $n$=3. *$P$=0.045, **$P$=0.048 (two-tailed *t*-test). All error bars represent s.e.m. (**C-F**) Histological analysis of the OFT of *Bmp4/7* dCKO and *miR-17-92* overexpression embryos at E10.5. Black and white arrowheads indicate proximal and distal OFT mesenchymal cells, respectively. ba, branchial arch; m, myocardium; mc, mesenchymal cushion; e, epithelium. Scale bars: 100 μm. (**G**) Regulation of OFT development by Bmp. Solid lines indicate direct regulation; broken lines indicate genetic regulation.

**Table 2. OFT mesenchymal phenotype of the *Bmp4/7* mutant**

| Genotype | Proximal OFT | Distal OFT |
|---|---|---|
| *Mef2c-Cre;Bmp4/7$^{f/f}$* | 1/17 | 6/17 |
| *Mef2c-Cre;Bmp4/7$^{f/f}$;miR-17-92$^{OE/+}$* | 5/6 | 6/6 |

The occurrence of mesenchymal cushion cells in the proximal and distal OFT among total embryos examined is shown for each genotype.

in endocardial cells disrupts OFT development, with abnormal cushion morphogenesis (Zhou et al., 2012). This indicates that endocardium is a target cell for Vegf signaling. There are no previous findings implicating Vegfa signaling in CNC development. Our data suggest that elevated Vegfa inhibits CNC influx into the OFT; however, more experiments are required to confirm this.

## A mechanism to tightly modulate Vegfa activity in the developing heart

Previous genetic studies have shown that the Vegfa dose must be maintained within a narrow window for normal embryonic development. *Vegfa* heterozygosity, as well as small gains in Vegfa activity, result in defective embryonic development. Loss of a single *Vegfa* allele is embryonic lethal at mid-gestation due to impaired angiogenesis and blood island formation (Ferrara et al., 1996). Moreover, there are cardiomyoblast differentiation defects in *Vegfa* heterozygotes. Haigh et al. found that heterozygous inactivation of *Vegfa* using *Col2a1-Cre* caused lethality at E10.5, with defects in the myocardial and endocardial layers of the heart (Haigh et al., 2000). A different *Vegfa* allele, *Vegf$^{hi}$*, results in 3-fold overexpression of *Vegfa* during development; heterozygotes for this allele are viable, whereas homozygous embryos die at E9.0 with dorsal aortae defects and severe abnormalities in yolk sac vasculature (Damert et al., 2002).

Our data indicate that Vegfa activity in the OFT is concurrently regulated by Smad transcriptional repression and post-transcriptional repression by miRNAs. Vegfa has previously been reported to be regulated by miRNAs, including the miR-17 family, in other contexts including cultured breast cancer cells and diabetes (Cascio et al., 2010; Long et al., 2010). However, our finding that miRNA regulation cooperates with Smad-mediated repression provides new insight into the mechanisms underlying tight Vegfa dosage regulation.

## Bmp interacts with calcineurin-NFAT signaling

Previous work indicated that *Nfatc1* mutants have conotruncal valve phenotypes similar to those of a *Mef2c-Cre;Bmp2/4/7* triple mutant (Y.B. and J.F.M., unpublished). Moreover, similar to what we have discovered for Bmp signaling, Nfatc1 inhibits *Vegfa* expression in the E9.5 OFT to permit EMT (Chang et al., 2004; Stankunas et al., 2010). Nfatc1 expression is reduced in the AV cushion endocardium of *Bmp2* conditional mutant embryos (Ma et al., 2005). There is evidence from pulmonary vascular cells that NFAT and Bmp are in a linear genetic pathway (Chan et al., 2011). Other intriguing data indicate that NFAT can promote chondrogenesis *in vitro*, a known function for Bmp signaling (Tomita et al., 2002). More work will be required to reveal potential interactions between calcineurin-NFAT and Bmp signaling in the developing OFT.

**Acknowledgements**
We thank Dr Stephanie Greene for discussions; and Dr Luis Luna-Zurita and Dr José Luis de la Pompa (Laboratorio de Biología Celular y del Desarrollo) for the explant culture protocol.

**Funding**
This work was supported by National Institutes of Health grants [R01HL093484 and R01DE12324] and Vivian L. Smith Foundation (J.F.M.); by an American Heart Association Southwest Affiliate Predoctoral Fellowship [#12PRE11720003 to Y.B.]; by an American Heart Association Scientist Development Grant [0930240N to Y.M.]; and by the Heart Rhythm Society (J.W.). Deposited in PMC for release after 12 months.

**Competing interests statement**
The authors declare no competing financial interests.

**Author contributions**
Y.B. and J.F.M. designed research; Y.B., J.W., Y.M., M.B.-C. and E.K. performed research; Y.B. and J.F.M. analyzed data; and Y.B., Y.M., and J.F.M. wrote the paper.

**Supplementary material**
Supplementary material available online at
http://dev.biologists.org/lookup/suppl/doi:10.1242/dev.097360/-/DC1

**References**

**Bonilla-Claudio, M., Wang, J., Bai, Y., Klysik, E., Selever, J. and Martin, J. F.** (2012). Bmp signaling regulates a dose-dependent transcriptional program to control facial skeletal development. *Development* **139**, 709-719.
**Bruneau, B. G.** (2008). The developmental genetics of congenital heart disease. *Nature* **451**, 943-948.
**Cascio, S., D'Andrea, A., Ferla, R., Surmacz, E., Gulotta, E., Amodeo, V., Bazan, V., Gebbia, N. and Russo, A.** (2010). miR-20b modulates VEGF expression by targeting HIF-1 α and STAT3 in MCF-7 breast cancer cells. *J. Cell. Physiol.* **224**, 242-249.
**Chan, M. C., Weisman, A. S., Kang, H., Nguyen, P. H., Hickman, T., Mecker, S. V., Hill, N. S., Lagna, G. and Hata, A.** (2011). The amiloride derivative phenamil attenuates pulmonary vascular remodeling by activating NFAT and the bone morphogenetic protein signaling pathway. *Mol. Cell. Biol.* **31**, 517-530.
**Chang, C.-P., Neilson, J. R., Bayle, J. H., Gestwicki, J. E., Kuo, A., Stankunas, K., Graef, I. A. and Crabtree, G. R.** (2004). A field of myocardial-endocardial NFAT signaling underlies heart valve morphogenesis. *Cell* **118**, 649-663.
**Damert, A., Miquerol, L., Gertsenstein, M., Risau, W. and Nagy, A.** (2002). Insufficient VEGFA activity in yolk sac endoderm compromises haematopoietic and endothelial differentiation. *Development* **129**, 1881-1892.
**Davis, B. N., Hilyard, A. C., Lagna, G. and Hata, A.** (2008). SMAD proteins control DROSHA-mediated microRNA maturation. *Nature* **454**, 56-61.
**Diman, N. Y. S. G., Remacle, S., Bertrand, N., Picard, J. J., Zaffran, S. and Rezsohazy, R.** (2011). A retinoic acid responsive Hoxa3 transgene expressed in embryonic pharyngeal endoderm, cardiac neural crest and a subdomain of the second heart field. *PLoS ONE* **6**, e27624.
**Dudley, A. T. and Robertson, E. J.** (1997). Overlapping expression domains of bone morphogenetic protein family members potentially account for limited tissue defects in BMP7 deficient embryos. *Dev. Dyn.* **208**, 349-362.
**Ferrara, N., Carver-Moore, K., Chen, H., Dowd, M., Lu, L., O'Shea, K. S., Powell-Braxton, L., Hillan, K. J. and Moore, M. W.** (1996). Heterozygous embryonic lethality induced by targeted inactivation of the VEGF gene. *Nature* **380**, 439-442.
**Furuta, Y., Piston, D. W. and Hogan, B. L.** (1997). Bone morphogenetic proteins (BMPs) as regulators of dorsal forebrain development. *Development* **124**, 2203-2212.
**Haigh, J. J., Gerber, H. P., Ferrara, N. and Wagner, E. F.** (2000). Conditional inactivation of VEGF-A in areas of collagen2a1 expression results in embryonic lethality in the heterozygous state. *Development* **127**, 1445-1453.
**Itoh, S., Itoh, F., Goumans, M.-J. and Ten Dijke, P.** (2000). Signaling of transforming growth factor-β family members through Smad proteins. *Eur. J. Biochem.* **267**, 6954-6967.
**Karaulanov, E., Knöchel, W. and Niehrs, C.** (2004). Transcriptional regulation of BMP4 synexpression in transgenic Xenopus. *EMBO J.* **23**, 844-856.
**Kawabata, M., Imamura, T. and Miyazono, K.** (1998). Signal transduction by bone morphogenetic proteins. *Cytokine Growth Factor Rev.* **9**, 49-61.
**Koralov, S. B., Muljo, S. A., Galler, G. R., Krek, A., Chakraborty, T., Kanellopoulou, C., Jensen, K., Cobb, B. S., Merkenschlager, M., Rajewsky, N. et al.** (2008). Dicer ablation affects antibody diversity and cell survival in the B lymphocyte lineage. *Cell* **132**, 860-874.
**Liu, W., Selever, J., Wang, D., Lu, M.-F., Moses, K. A., Schwartz, R. J. and Martin, J. F.** (2004). Bmp4 signaling is required for outflow-tract septation and branchial-arch artery remodeling. *Proc. Natl. Acad. Sci. USA* **101**, 4489-4494.
**Long, J., Wang, Y., Wang, W., Chang, B. H. J. and Danesh, F. R.** (2010). Identification of microRNA-93 as a novel regulator of vascular endothelial growth factor in hyperglycemic conditions. *J. Biol. Chem.* **285**, 23457-23465.

**Lu, M.-F., Pressman, C., Dyer, R., Johnson, R. L. and Martin, J. F.** (1999). Function of Rieger syndrome gene in left-right asymmetry and craniofacial development. *Nature* **401**, 276-278.
**Luna-Zurita, L., Prados, B., Grego-Bessa, J., Luxán, G., del Monte, G., Benguría, A., Adams, R. H., Pérez-Pomares, J. M. and de la Pompa, J. L.** (2010). Integration of a Notch-dependent mesenchymal gene program and Bmp2-driven cell invasiveness regulates murine cardiac valve formation. *J. Clin. Invest.* **120**, 3493-3507.
**Ma, L., Lu, M.-F., Schwartz, R. J. and Martin, J. F.** (2005). Bmp2 is essential for cardiac cushion epithelial-mesenchymal transition and myocardial patterning. *Development* **132**, 5601-5611.
**McCulley, D. J., Kang, J.-O., Martin, J. F. and Black, B. L.** (2008). BMP4 is required in the anterior heart field and its derivatives for endocardial cushion remodeling, outflow tract septation, and semilunar valve development. *Dev. Dyn.* **237**, 3200-3209.
**Niessen, K., Fu, Y., Chang, L., Hoodless, P. A., McFadden, D. and Karsan, A.** (2008). Slug is a direct Notch target required for initiation of cardiac cushion cellularization. *J. Cell Biol.* **182**, 315-325.
**Olson, E. N.** (2006). Gene regulatory networks in the evolution and development of the heart. *Science* **313**, 1922-1927.
**Shi, Y. and Massagué, J.** (2003). Mechanisms of TGF-β signaling from cell membrane to the nucleus. *Cell* **113**, 685-700.
**Shi, Y., Wang, Y. F., Jayaraman, L., Yang, H., Massagué, J. and Pavletich, N. P.** (1998). Crystal structure of a Smad MH1 domain bound to DNA: insights on DNA binding in TGF-beta signaling. *Cell* **94**, 585-594.
**Solloway, M. J. and Robertson, E. J.** (1999). Early embryonic lethality in Bmp5;Bmp7 double mutant mice suggests functional redundancy within the 60A subgroup. *Development* **126**, 1753-1768.
**Stankunas, K., Ma, G. K., Kuhnert, F. J., Kuo, C. J. and Chang, C.-P.** (2010). VEGF signaling has distinct spatiotemporal roles during heart valve development. *Dev. Biol.* **347**, 325-336.
**Tomita, M., Reinhold, M. I., Molkentin, J. D. and Naski, M. C.** (2002). Calcineurin and NFAT4 induce chondrogenesis. *J. Biol. Chem.* **277**, 42214-42218.
**Ventura, A., Young, A. G., Winslow, M. M., Lintault, L., Meissner, A., Erkeland, S. J., Newman, J., Bronson, R. T., Crowley, D., Stone, J. R. et al.** (2008). Targeted deletion reveals essential and overlapping functions of the miR-17 through 92 family of miRNA clusters. *Cell* **132**, 875-886.
**Verzi, M. P., McCulley, D. J., De Val, S., Dodou, E. and Black, B. L.** (2005). The right ventricle, outflow tract, and ventricular septum comprise a restricted expression domain within the secondary/anterior heart field. *Dev. Biol.* **287**, 134-145.
**Wang, J., Greene, S. B., Bonilla-Claudio, M., Tao, Y., Zhang, J., Bai, Y., Huang, Z., Black, B. L., Wang, F. and Martin, J. F.** (2010). Bmp signaling regulates myocardial differentiation from cardiac progenitors through a MicroRNA-mediated mechanism. *Dev. Cell* **19**, 903-912.
**Williams, J. M., de Leeuw, M., Black, M. D., Freedom, R. M., Williams, W. G. and McCrindle, B. W.** (1999). Factors associated with outcomes of persistent truncus arteriosus. *J. Am. Coll. Cardiol.* **34**, 545-553.
**Xiao, C., Srinivasan, L., Calado, D. P., Patterson, H. C., Zhang, B., Wang, J., Henderson, J. M., Kutok, J. L. and Rajewsky, K.** (2008). Lymphoproliferative disease and autoimmunity in mice with increased miR-17-92 expression in lymphocytes. *Nat. Immunol.* **9**, 405-414.
**Yamagishi, H., Maeda, J., Uchida, K., Tsuchihashi, T., Nakazawa, M., Aramaki, M., Kodo, K. and Yamagishi, C.** (2009). Molecular embryology for an understanding of congenital heart diseases. *Anat. Sci. Int.* **84**, 88-94.
**Yang, J., Mani, S. A., Donaher, J. L., Ramaswamy, S., Itzykson, R. A., Come, C., Savagner, P., Gitelman, I., Richardson, A. and Weinberg, R. A.** (2004). Twist, a master regulator of morphogenesis, plays an essential role in tumor metastasis. *Cell* **117**, 927-939.
**Zhao, Y. and Srivastava, D.** (2007). A developmental view of microRNA function. *Trends Biochem. Sci.* **32**, 189-197.
**Zhou, J., Pashmforoush, M. and Sucov, H. M.** (2012). Endothelial neuropilin disruption in mice causes DiGeorge syndrome-like malformations via mechanisms distinct to those caused by loss of Tbx1. *PLoS ONE* **7**, e32429.
**Zwijsen, A., Verschueren, K. and Huylebroeck, D.** (2003). New intracellular components of bone morphogenetic protein/Smad signaling cascades. *FEBS Lett.* **546**, 133-139.